

High-Power, High-Speed Photodiodes

The primary goal of this program was to design MUTC photodiodes optimized for the frequency bands to be employed in the Next Generation Very Large Array. This was carried out in collaboration with Bill Shillue at the NRAO Central Development Laboratory.

To achieve high RF output power at high frequency, various photodiode structures have been developed among which the uni-traveling carrier (UTC) structure [1,2] has demonstrated high saturation current at high frequency. In an InGaAs/InP UTC photodiode, photons excite carriers in an undepleted p-type InGaAs absorption layer. Since only electrons are injected into the InP drift layer, the effective transit time is shorter than for a p-i-n structure, which has both electrons and holes in the drift region, and there is minimal space charge screening effect. The UTC structure has been modified to further reduce the space-charge effect while maintaining high bandwidth. A schematic cross section of the structure is shown in Fig. 2. By inserting an undoped InGaAs layer with an appropriate thickness between the undepleted InGaAs absorption layer and the InP drift layer,

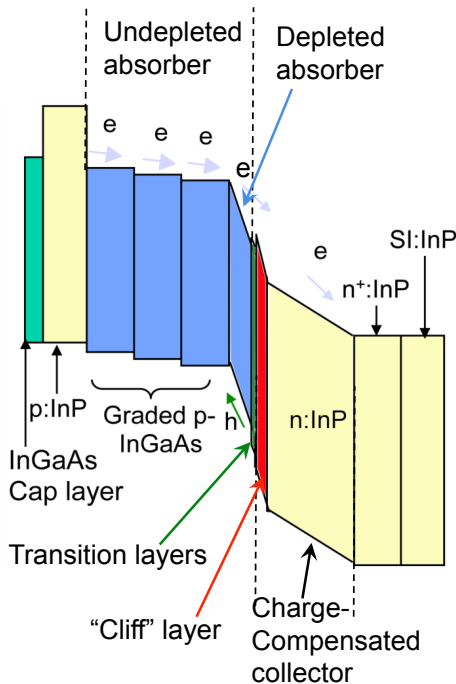


Figure 2. Modified charge-compensated uni-traveling carrier (MUTC) photodiode with cliff layer

By inserting an undoped InGaAs layer with an appropriate thickness between the undepleted InGaAs absorption layer and the InP drift layer, the responsivity of the UTC PD can be increased [3]. Of greater benefit, this layer also helps to maintain high electric field at the heterojunction interfaces, which facilitates electron transport. The RF output power can also be increased by incorporating a lightly doped charge in the depletion region [4], which pre-distorts the electric field to partially compensate the field change caused by the space charge effect. Finally, adding a charge layer or “cliff” layer [5], enhances the electric field next to the absorption region, which suppresses field collapse in the depleted absorber layer. These structures, referred to as modified uni-traveling carrier (MUTC) photodiodes, have proved so successful at suppressing the space-charge effect that thermal failure has become the primary factor that limits the maximum operating current.

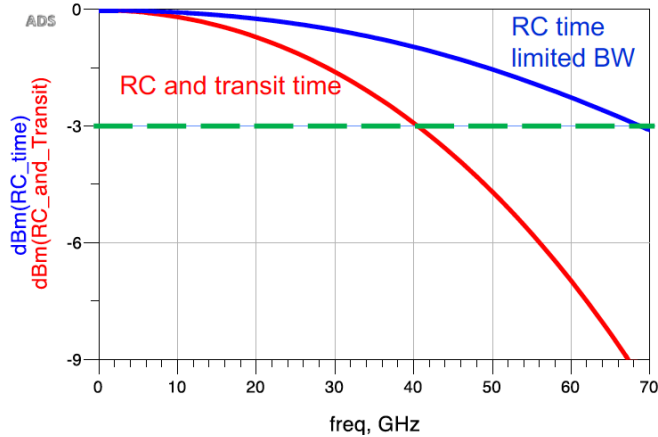
The surface temperature of a conventional backside-illuminated photodiode was measured by thermo-reflectance imaging [6]. For power dissipation of 500 mW it was found that the surface temperature can reach 500 K. An optical probe technique that measures the temperature inside the photodiode has shown that the temperature in the depletion region may be ~ 100K higher than the surface temperature [7]. Among the various techniques to improve thermal dissipation, flip-chip bonding has achieved the best results [8-11]. However, it is important to note that there are tradeoffs in the performance parameters that affect the structural design. For example, in order to increase the bandwidth, it is necessary to reduce the thickness of the absorption region in order to decrease the electron and hole transit times. That results in decreased quantum efficiency

(responsivity). The thinner absorber also tends to increase the capacitance, which necessitates reducing the device diameter. This results in higher current densities, lower failure current, and lower RF output power.

We completed our design of high-power photodiodes for the three frequency bands that may be employed for the ngVLA, 10 – 40 GHz, 40 – 65 GHz, and 75 – 110 GHz. The structures and projected performance are summarized in the following:

10 GHz ~ 40 GHz Design

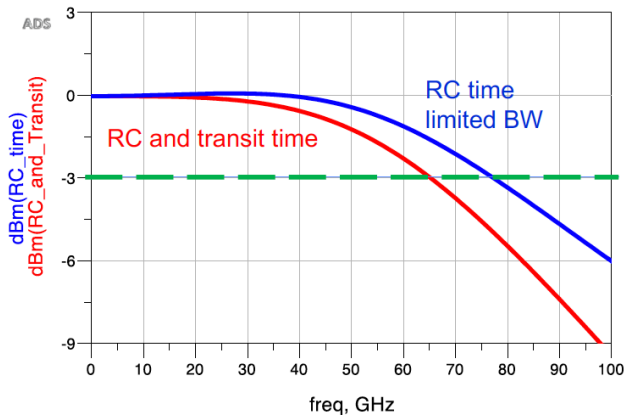
Contact layer InGaAs, p+, Zn, 2×10^{19} , 50nm
InP, p+, Zn, 2×10^{18} , 100nm
Grading InGaAsP, Q1.1, p+, Zn, 5×10^{18} , 15nm
Grading InGaAsP, Q1.4, p+, Zn, 5×10^{18} , 15nm
Un-depleted absorber InGaAs, p+, Zn, 2×10^{18} , 100nm
Un-depleted absorber InGaAs, p+, Zn, 1.2×10^{18} , 150nm
Un-depleted absorber InGaAs, p+, Zn, 8×10^{17} , 200nm
Un-depleted absorber InGaAs, p+, Zn, 5×10^{17} , 250nm
Depleted absorber InGaAs, n-, Si, 1×10^{16} , 350nm
Grading InGaAsP, Q1.4, n-, Si, 1×10^{15} , 15nm
Grading InGaAsP, Q1.1, n-, Si, 1×10^{15} , 15nm
Cliff layer InP, n-, Si, 1.4×10^{17} , 50nm
Drift layer InP, n-, Si, 1×10^{15} , 700nm
InP, n+, Si, 1.0×10^{18} , 100nm
InP, n+, Si, 1.0×10^{19} , 900nm
InP, semi-insulating substrate, Double side polished



- 24- μ m diameter MUTC-K device exhibits 40 GHz bandwidth with inductive peaking
 - CPW design: W:30 μ m, G: 200 μ m, L: 90 μ m
- The estimated transit-time bandwidth is 47 GHz (9 ps transit time).
- Estimated R: 0.97 A/W (with AR coating and top metal mirror with backside illumination)

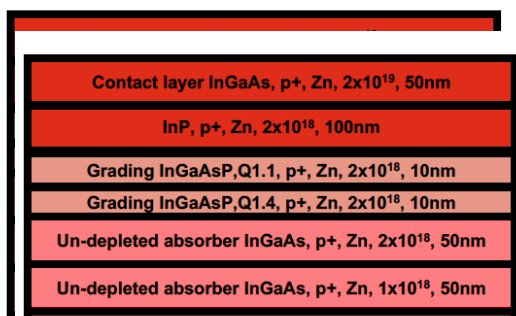
40 GHz ~ 65 GHz device design

Contact layer InGaAs, p+, Zn, 2×10^{19} , 50nm
InP, p+, Zn, 2×10^{18} , 100nm
Grading InGaAsP, Q1.1, p+, Zn, 5×10^{18} , 15nm
Grading InGaAsP, Q1.4, p+, Zn, 5×10^{18} , 15nm
Un-depleted absorber InGaAs, p+, Zn, 2×10^{18} , 100nm
Un-depleted absorber InGaAs, p+, Zn, 1.2×10^{18} , 150nm
Un-depleted absorber InGaAs, p+, Zn, 8×10^{17} , 150nm
Depleted absorber InGaAs, n-, Si, 1×10^{16} , 250nm
Grading InGaAsP, Q1.4, n-, Si, 1×10^{15} , 15nm
Grading InGaAsP, Q1.1, n-, Si, 1×10^{15} , 15nm
Cliff layer InP, n-, Si, 1.4×10^{17} , 50nm
Drift layer InP, n-, Si, 1×10^{15} , 400nm
InP, n+, Si, 1.0×10^{18} , 100nm
InP, n+, Si, 1.0×10^{19} , 900nm
InP, semi-insulating substrate, Double side polished

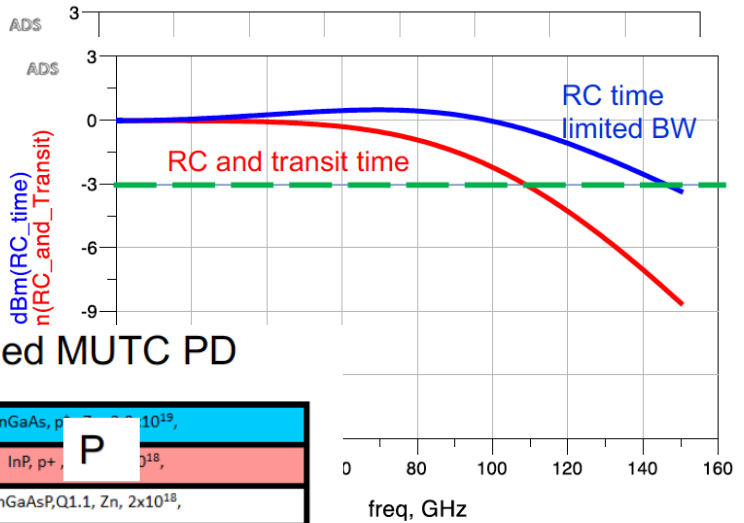


- 18- μ m diameter MUTC-V device exhibits 65 GHz bandwidth with inductive peaking
 - CPW design: W:25 μ m, G: 220 μ m, L: 140 μ m
- The estimated transit-time bandwidth is 72 GHz (6 ps transit time).
- Estimated R: 0.76 A/W (with AR coating and top metal mirror with backside illumination)

75 GHz ~ 110 GHz



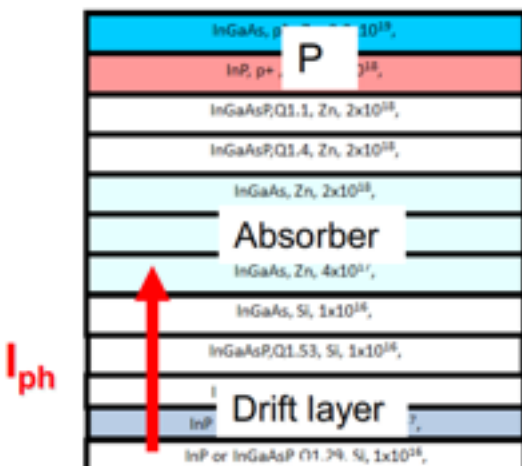
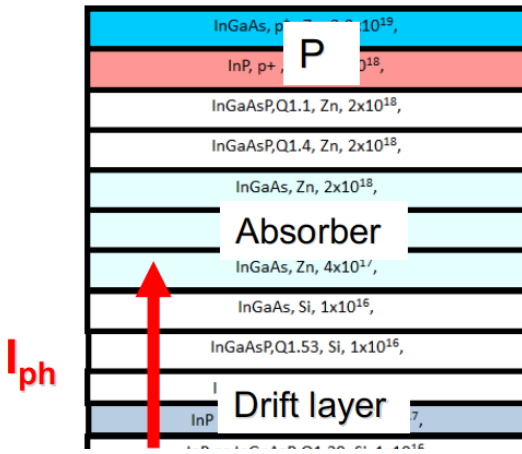
Evanescently coupled MUTC PD



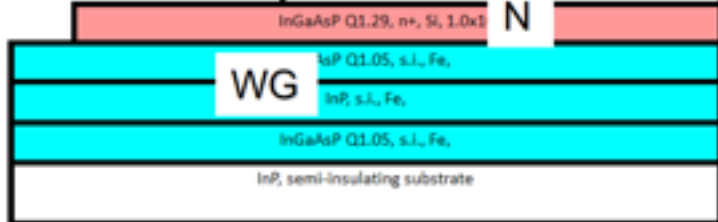
-W device exhibits 110 GHz
e peaking
0 μm, G: 200 μm, L: 100 μm
me bandwidth is 117 GHz (3.8
(with AR coating and top
side illumination)

Optical

Evanescently coupled MUTC PD



Optical input



Our simulations project a responsivity of 0.67 A/W for a 50 μm² device with a bandwidth of 110 GHz, which is ~ 60% improvement compared to a surface-normal device. These devices have not been fabricated as wafer costs and laboratory fees exceed the budget for this program. However, it appears that significant improvements compared to previous reports can be achieved. In summary, we demonstrated a pathway to increase the bandwidth and responsivity of

photodiodes for analog links without sacrificing RF output power. This was accomplished by modifying the design to increase the transit times since the bandwidths were RC limited in earlier structures. This resulted in lower capacitance, which in turn enabled us to use larger diameters for a given bandwidth. Larger device diameters lead to higher RF output power. Increasing the layer thicknesses also resulted in higher responsivities. Most recently, for the highest bandwidth photodiodes, we have investigated waveguide photodiodes that can achieve higher responsivity by coupling light into a waveguide that evanescently transitions the signal to the detector.

References

- ¹ T. Ishibashi, N. Shimizu, S. Kodama, H. Ito, T. Nagatsuma and T. Furuta, *Tech. Dig. Ultrafast Electronics and Optoelectronics*, p.83-87, 1997.
- ² H. Ito, H. Fushimi, Y. Muramoto, T. Furuta, and T. Ishibashi, *J. Lightwave Tech.*, **20**(8), , p. 1500-1505, 2002.
- ³ X. Wang, N. Duan, H. Chen, and J. C. Campbell, *IEEE Photon. Tech. Lett.*, **19**(16), p. 1272-1274, Aug. 2007.
- ⁴ N. Li, X. Li, S. Demiguel, X. Zheng, J.C. Campbell, D.A. Tulchinsky, K.J. Williams, T.D. Isshiki, G.S. Kinsey and R. Sudharsansan, *IEEE Photon. Technol. Lett.*, vol. 16, no. 3, pp. 864-866, 2004.
- ⁵ N. Shimizu, N. Watanabe, T. Furuta and T. Ishibashi, *IEEE Photon. Technol. Lett.*, vol. 10, no. 3, pp. 412-414, 1998.
- ⁶ Z. Li, Y. Fu, M. Piels, H. Pan, A. Beling, J. E. Bowers, and J. C. Campbell, *Optics Express*, 19(26), p. B385-B390, 2011.
- ⁷ H. Chen, A. Beling, H. Pan, and J. C. Campbell, *IEEE J. Quantum Electronics*, **45**(12), p. 1537-1541, Dec. 2009.
- ⁸ A. Beling, A. S. Cross, Q. Zhou, Y. Fu, and J. C. Campbell, in *Photonics Conference (IPC) 2013 (IEEE 2013)*, p. 352-353.
- ⁹ A. S. Cross, Q. Zhou, A. Beling, Y. Fu, and J. C. Campbell, *Opt Express* **21**, 9967-9973 (2013).
- ¹⁰ Q. Zhou, A. S. Cross, A. Beling, Y. Fu, Z. W. Lu, and J. C. Campbell, *IEEE Photonics Technol. Lett.* **25**, p. 907-909 (2013).
- ¹¹ Xiaojun Xie, Qiugui Zhou, Kejia Li, Yang Shen, Qinglong Li, Zhanyu Yang, Andreas Beling, and Joe C. Campbell, *Optica*, **1**(6), p. 429 – 436, 2014.

The National Radio Astronomy Observatory and Green Bank Observatory are facilities of the U.S. National Science Foundation operated under cooperative agreement by Associated Universities, Inc. This work was supported by awards AST-2034328 (MSIP Prototype Antenna) and AST-2334267 (ngVLA Design Activities); NRAO related activities are funded under award AST-1647378 (NRAO Operations/Development).

